

## Dip-pen nanolithography with magnetic $\text{Fe}_2\text{O}_3$ nanocrystals

Gautam Gundiah, Neena Susan John, P. John Thomas, G. U. Kulkarni, and C. N. R. Rao<sup>a)</sup>  
*Chemistry and Physics of Materials Unit, Jawaharlal Nehru Centre for Advanced Scientific Research,  
Jakkur, Bangalore-560064, India*

S. Heun

*Sincrotrone Trieste S. c. p. a., I-34012 Trieste, Italy*

(Received 18 March 2004; accepted 4 May 2004; published online 17 June 2004)

Dip-pen nanolithography has been employed to obtain magnetic nanopatterns of  $\gamma\text{-Fe}_2\text{O}_3$  nanocrystals on mica and silicon substrates. The chemical and magnetic nature of the patterns have been characterized employing low-energy electron microscopy, x-ray photoemission electron microscopy, and magnetic force microscopy measurements. © 2004 American Institute of Physics.  
[DOI: 10.1063/1.1766399]

Dip-pen nanolithography (DPN), an atomic force microscopy (AFM)-based lithographic technique, developed by Mirkin and co-workers,<sup>1</sup> is emerging as a preferred method to create patterns of nanoscopic dimensions. The method exploits the water meniscus formed between a slowly scanning AFM tip and a substrate to transfer the species on the tip to the substrate by diffusion. Initial studies employed gold–thiol interaction to create robust patterns, with the dimensions being determined by the preset scan area.<sup>2</sup> The use of bifunctional thiols as inks permits tethering of colloids, proteins, and other macromolecules at specific regions on a given surface.<sup>3</sup> Ali *et al.*<sup>4</sup> have reported a DPN-based procedure to deposit small volumes of an Au sol on a substrate, which on evaporation of the solvent leads to circular nanocrystal patterns. Garno *et al.*<sup>5</sup> have suggested methods to obtain linear patterns of Au nanocrystals on Au substrates. DPN patterning of Au and Pd nanocrystals has been accomplished on different substrates starting from hydrosols.<sup>6</sup> Magnetic barium hexaferrite nanostructures have been patterned by coating the AFM cantilever tip with a precursor followed by its deposition on silicon substrates and heating.<sup>7</sup> Based on DPN experiments on organic dyes, Su and Dravid<sup>8</sup> suggest that weak interactions between the substrate and the molecular ink suffice to form DPN patterns. In spite of the progress made with DPN, there is a clear need to develop better inks for different surfaces and fully characterize the nanopatterns by appropriate spectroscopic and microscopic tools.<sup>9</sup>

We have sought to pattern nanoparticles of  $\gamma\text{-Fe}_2\text{O}_3$  by the DPN method on different substrates. It may be interesting to recall that hematite has been traditionally employed as a dye, the prehistoric cave paintings of Lascaux, being a well-known example. Since  $\gamma\text{-Fe}_2\text{O}_3$  is magnetic, the nanopatterns also lend themselves to a magnetic force microscopy (MFM) study. In this letter, we report DPN with  $\gamma\text{-Fe}_2\text{O}_3$  nanoparticles wherein MFM as well as low-energy electron microscopy (LEEM) and x-ray photoemission electron microscopy (XPEEM) (Ref. 10) have been employed to independently characterize the patterns.

Citrate-capped  $\gamma\text{-Fe}_2\text{O}_3$  nanocrystals were prepared by wet-chemical means, by modifying the procedure of Ngo and Pileni.<sup>11</sup> The preparation yields a sol, which can be precipi-

tated and redispersed readily in water. Redispersibility is crucial for a colloidal sol to be used as an ink in DPN experiments. The transmission electron microscopy (TEM) image [see Fig. 1(a)], revealed the nanocrystals to be of an average diameter of 11 nm and a log-normal diameter distribution [see inset in Fig. 1(a)]. The nanocrystals in the powder form were superparamagnetic at room temperature, exhibiting hysteresis at low temperatures [see Fig. 1(b)]. The observed squareness ratio of 0.42 is close to that expected (0.5) for randomly oriented single domain magnetic particles with uniaxial anisotropy.<sup>12</sup>

DPN experiments were carried out under ambient conditions (humidity ~35%–45%) by employing a Digital Instruments Multimode head attached to a Nanoscope-IV controller. Contact mode imaging was carried out in both normal and lateral force modes. Standard  $\text{Si}_3\text{Ni}_4$  cantilevers were coated with  $\gamma\text{-Fe}_2\text{O}_3$  nanocrystals by immersing them in a dispersion for 5–10 min followed by drying. Freshly cleaved mica and silicon were used as substrates with and without the native  $\text{SiO}_x$  layer (the latter by treating with a solution of aqueous HF). Deposition of the nanocrystals was achieved by scanning an area in the contact mode with scan speeds of  $\sim 1 \mu\text{m s}^{-1}$  for a period of 30 min. Subsequently, imaging was carried out using the same cantilever and scanning a larger area with higher scan rates ( $\sim 10 \mu\text{m s}^{-1}$ ).

The AFM images in Fig. 2 clearly show that patterns of  $\gamma\text{-Fe}_2\text{O}_3$  nanocrystals can be fabricated satisfactorily on different substrates. In each case, high aspect ratio lines, corresponding to the desired scan area are obtained with sharp edges. For example, scanning an area of 9000 nm by 230 nm during deposition produced a pattern of dimensions 9010 nm by 226 nm [Fig. 2(a), central line]. Typical linewidths are in the range of 140–200 nm with lengths extending to 10  $\mu\text{m}$ . It is gratifying that there is no sign of lateral diffusion of the ink in any of the cases. These patterns are therefore distinct from water droplets that are deposited from undipped tips.<sup>13</sup> The water droplets evaporate readily and exhibit noncontinuous structures with diffuse boundaries. The surface plot shown in Fig. 2(b) confirms the observations made in Fig. 2(a). We also see corrugations along the edges corresponding to the particle size. The individual particles are not visible in the patterns, possibly due to the blunt nature of the cantilever coated with the nanocrystals and also due to the mild contact forces employed. The observed height of around 10 nm re-

<sup>a)</sup> Author to whom correspondence should be addressed; electronic mail: cnrao@jncasr.ac.in

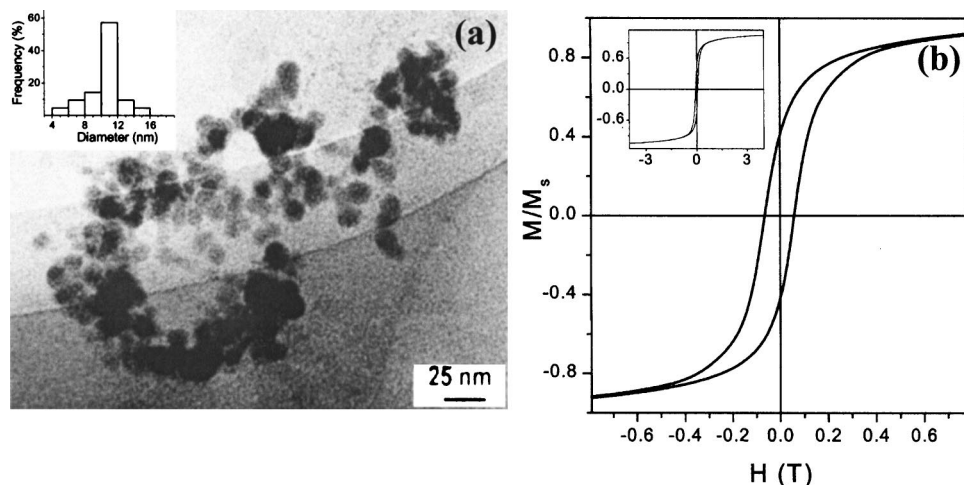


FIG. 1. Citrate-capped  $\gamma\text{-Fe}_2\text{O}_3$  nanocrystals: (a) TEM image along with a histogram showing the distribution in particle size (in the inset) and (b) hysteresis loop at 2 K ( $H=4$  T). The inset shows the hysteresis loop in the full range of the magnetic field.

veals that the patterns are made of a single layer of  $\gamma\text{-Fe}_2\text{O}_3$  nanocrystals. It is noteworthy that similar lines are obtained on Si with and without the native oxide layer, although the latter is not ideal for good imaging [see Figs. 2(c) and 2(d)].

The magnetic behavior of the nanopatterns was probed by magnetic cantilever tips, the magnetic nature of the  $\gamma\text{-Fe}_2\text{O}_3$  nanocrystals being exploited to obtain MFM contrast. In this method, a magnetic tip is scanned in the lift mode,<sup>14</sup> at various  $z$  values, wherein the magnetic interaction emerges as a difference in the phase shift. Typical tapping mode topography and MFM images are shown in Figs. 3(a) and 3(b). The tapping mode reveals rougher edges arising from the nanocrystals. The change in the phase shift as function of the lift height is shown in Fig. 3(c), to show that the superparamagnetic nanocrystals in the pattern are susceptible to magnetization by the stray field emanating from the magnetic tip. The loss of contrast upon changing the lift height to 10 nm is consistent with the rather weak magnetic nature of the nanocrystals [see Fig. 1(b)].

In order to characterize the DPN patterns by an independent method, we have employed the Nanospectroscopy

Beamline at the synchrotron radiation facility Elettra in Trieste.<sup>15</sup> Electron-beam-based techniques are ideal for such studies<sup>16</sup> in that they have a lateral resolution of 10 nm and atomic depth resolution. In LEEM, a low-energy electron beam is incident on the sample and the backscattered beam is used for imaging in the dark or bright field. The image of Fig. 4(b) was acquired in the mirror electron microscopy (MEM) mode wherein the sample potential is negative with respect to the filament so that the electrons are reflected by the surface potential in front of the sample, causing minimal damage to the nanocrystals. The contrast itself arises from variation in the surface potential and topography. These studies were carried out typically a few weeks after patterning of the nanocrystals on Si surfaces with native oxide layers, demonstrating thereby that the patterns are robust. The patterns were located on the substrates by using suitable micron-sized markers. In Figs. 4(a) and 4(b), we compare the LEEM image in the MEM mode along with the corresponding AFM image obtained right after patterning. The LEEM image corresponds exactly with the AFM image.

We have ascertained the chemical nature of the species by imaging the nanopattern by an independent method, we have recorded XPEEM images. The image in Fig. 4(c) was obtained in x-ray absorption spectroscopy mode with a photon energy of 712 eV using secondary electrons for imaging

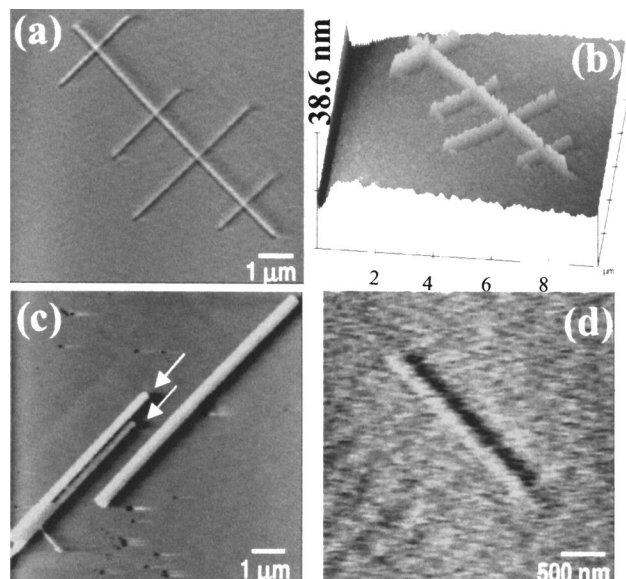


FIG. 2. Contact AFM images of  $\gamma\text{-Fe}_2\text{O}_3$  nanocrystal patterns drawn (a) on mica along with (b) its surface plot, (c) on silicon with the native  $\text{SiO}_x$  layer (arrows point to closely-drawn patterns) and (d) on etched silicon.

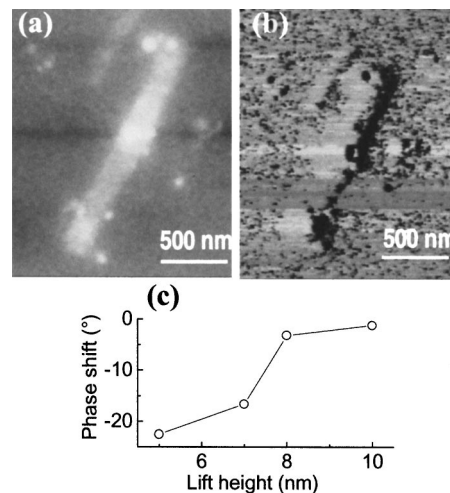


FIG. 3. (a) Tapping mode AFM image of a  $\gamma\text{-Fe}_2\text{O}_3$  nanopattern, (b) the corresponding MFM image at a lift height of 5 nm and (c) plot of the phase shift vs the lift height.

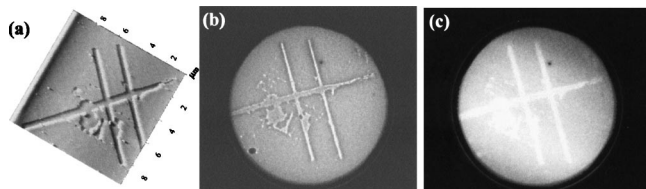


FIG. 4. (a) Tapping mode topographic AFM image of a  $\gamma$ -Fe<sub>2</sub>O<sub>3</sub> nanocrystal pattern along with (b) the corresponding MEM image collected with electron beam of energy 0.8 eV and (c) XPEEM image obtained by collecting the secondary electrons (energy 0.6 eV) following excitation with 712 eV (Fe  $L_3$  edge). The field of view in both cases is 10  $\mu$ m.

(electron energy 0.6 eV). The photon energy corresponds to the excitation of the Fe  $L_3$  edge in Fe<sub>2</sub>O<sub>3</sub> as verified with a bulk reference sample. The image obtained with photoelectrons corresponds exactly to the AFM image.

In conclusion, we have demonstrated a versatile DPN method for nanopatterning  $\gamma$ -Fe<sub>2</sub>O<sub>3</sub> nanocrystals on different substrates. The patterns are well defined with minimal lateral diffusion of the ink. The patterns are also magnetic and yields well-resolved LEEM and XPEEM images.

The authors thank the Department of Science and Technology, Government of India, for support of this research. One of the authors (N.S.J.) thanks CSIR (India) for financial support.

- <sup>1</sup>D. S. Ginger, H. Zhang, and C. A. Mirkin, *Angew. Chem., Int. Ed.* **43**, 30 (2004) and references therein.
- <sup>2</sup>R. D. Piner, J. Zhu, F. Xu, S. Hong, and C. A. Mirkin, *Science* **283**, 661 (1999).
- <sup>3</sup>R. Mckendry, W. T. S. Huck, B. Weeks, M. Fiorini, C. Abell, and T. Rayment, *Nano Lett.* **2**, 713 (2002); L. M. Demers and C. A. Mirkin, *Angew. Chem., Int. Ed. Engl.* **40**, 3069 (2001); X. Liu, L. Fu, S. Hong, V. P. Dravid, and C. A. Mirkin, *Adv. Mater. (Weinheim, Ger.)* **14**, 231 (2002).
- <sup>4</sup>M. B. Ali, T. Ondarcuhu, M. Brust, and C. Joachim, *Langmuir* **18**, 872 (2002).
- <sup>5</sup>J. C. Garno, Y. Yang, N. A. Amro, S. Cruchon-Dupeyrat, S. Chen, and G. Y. Liu, *Nano Lett.* **3**, 3 (2003).
- <sup>6</sup>P. J. Thomas, G. U. Kulkarni, and C. N. R. Rao, *J. Mater. Chem.* **14**, 625 (2004).
- <sup>7</sup>L. Fu, X. Liu, Y. Zhang, V. P. Dravid, and C. M. Mirkin, *Nano Lett.* **3**, 757 (2003).
- <sup>8</sup>M. Su and V. P. Dravid, *Appl. Phys. Lett.* **80**, 4434 (2002).
- <sup>9</sup>C. A. Mirkin, *MRS Bull.* **26**, 535 (2001).
- <sup>10</sup>T. Schmidt, S. Heun, J. Slezak, J. Diaz, K. C. Prince, G. Lilienkamp, and E. Bauer, *Surf. Rev. Lett.* **5**, 1287 (1998).
- <sup>11</sup>A. T. Ngo and M. P. Pileni, *J. Phys. Chem. B* **105**, 53 (2001).
- <sup>12</sup>S. Chikuzumi and S. H. Charap, *Physics of Magnetism* (Wiley, New York, 1964).
- <sup>13</sup>J. Hu, X.-D. Xiao, D. F. Ogletree, and M. Salmeron, *Surf. Sci.* **344**, 221 (1995).
- <sup>14</sup>Digital Instruments, Santa Barbara, CA.
- <sup>15</sup>A. Locatelli, A. Bianco, D. Cocco, S. Cherifi, S. Heun, M. Marsi, A. Pasqualetto, and E. Bauer, *J. Phys. IV* **104**, 99 (2003).
- <sup>16</sup>M. Lazzarino, S. Heun, B. Ressel, K. C. Prince, P. Pingue, and C. Ascoli, *Appl. Phys. Lett.* **81**, 2842 (2002).